Current Research in Food Science 8 (2024) 100748

Contents lists available at ScienceDirect

Current Research in Food Science

journal homepage: www.sciencedirect.com/journal/current-research-in-food-science

Perspectives from CO+RE

Phenotypic characterization and genomic analysis of *Limosilactobacillus fermentum* phage

Can Zhang [a,b,c,1], Xingyu Quan [a,b,c,1], Weiqi Lian [a,b,c], Runze Liu [a,b,c], Qiannan Wen [a,b,c], Xia Chen [a,b,c,*]

[a] Key Laboratory of Dairy Biotechnology and Engineering, Ministry of Education, Inner Mongolia Agricultural University, 010018, PR China
[b] Key Laboratory of Dairy Products Processing, Ministry of Agriculture and Rural Affairs, Inner Mongolia Agricultural University, 010018, PR China
[c] Collaborative Innovative Center of Ministry of Education for Lactic Acid Bacteria and Fermented Dairy Products, Inner Mongolia Agricultural University, 010018, PR China

ARTICLE INFO

Handling Editor: Dr. Siyun Wang

Keywords:
Limosilactobacillus fermentum phage
Infective properties
Environmental stress tolerance
Adsorption characteristics
Genome analysis

ABSTRACT

Limosilactobacillus (L.) fermentum is widely utilized for its beneficial properties, but lysogenic phages can integrate into its genome and can be induced to enter the lysis cycle under certain conditions, thus accomplishing lysis of host cells, resulting in severe economic losses. In this study, a lysogenic phage, LFP03, was induced from *L. fermentum* IMAU 32510 by UV irradiation for 70 s. The electron microscopy showed that this phage belonged to *Caudoviricetes* class. Its genome size was 39,556 bp with a GC content of 46.08%, which includes 20 functional proteins. Compared with other *L. fermentum* phages, the genome of phage LFP03 exhibited deletions, inversions and translocations. Biological analysis showed that its optimal multiplicity of infection was 0.1, with a burst size of 133.5 ± 4.9 PFU/infective cell. Phage LFP03 was sensitive to temperature and pH value, with a survival rate of 48.98% at 50 °C. It could be completely inactivated under pH 2. The adsorption ability of this phage was minimally affected by temperature and pH value, with adsorption rates reaching 80% under all treated conditions. Divalent cations could accelerate phage adsorption, while chloramphenicol expressed little influence. This study might expand the related knowledge of *L. fermentum* phages, and provide some theoretical basis for improving the stability of related products and establishing phage control measures.

1. Introduction

Limosilactobacillus (*L.*) *fermentum*, as one of the common heterofermentative lactic acid bacteria (LAB), is the dominant microorganism in traditional fermented food products. It could metabolize lactose, galactose and other carbohydrates into lactic acid, acetic acid and other metabolites (Zhao et al., 2019; Sachetti et al., 2021). As reported, *L. fermentum* can not only improve the flavor of fermented food products, but also exhibit good resistance in the gastrointestinal tract, as well as play antimicrobial activity against pathogens, modulate intestinal microbiota and immune response (Ephrem et al., 2019; Zhang et al., 2021).

As microbial virus, phages widely exist in the environment and outnumber bacteria by a factor of ten (Cantu et al., 2020). Phages could be categorized into lysogenic and lytic ones. Unlike lytic phages, lysogenic phages could integrate their genome into the genome of the host strain, forming lysogenic bacteria. Under specific conditions (such as ultraviolet (UV) irradiation, mitomycin C (MMC)), the prophages could be induced into lytic cycles (Toit, 2019). Then, it could result in abnormal growth of starter cultures, leading to fermentation failure and causing serious economic losses. As reported in 2020, prophages are commonly found in starter cultures used in food fermentation (Pei et al., 2020). In 2022, Abraha et al. (2022) analyzed the genomes of 164 strains of *Bacillus subtilis*, and found that 123 strains contained complete prophage genes. Happel et al. (2022) conducted prophage prediction on 895 strains of *Lactobacillaceae*, and found 359 genomes contained complete prophage genes.

To date, the whole genome sequences of 112 *Lactobacillus* phages have been published in NCBI, of which only 6 are *L. fermentum* phages (Lv et al., 2023a). As we known, the genomic and biological

* Corresponding author. Key Laboratory of Dairy Biotechnology and Engineering, Ministry of Education, Inner Mongolia Agricultural University, 306 Zhaowuda Road, Hohhot, 010018, PR China.
E-mail address: chenxia8280@163.com (X. Chen).
[1] These authors contributed equally to this work.

https://doi.org/10.1016/j.crfs.2024.100748
Received 7 January 2024; Received in revised form 14 April 2024; Accepted 22 April 2024
Available online 27 April 2024

characteristics of different phages are specific, and the library of *L. fermentum* lysogenic phages needs to be expanded. The aim of this study was to induce lysogenic phage under various conditions and evaluate the biological properties (such as infective properties, tolerance, and adsorption characteristics) and genome characteristics of the induced phage. This study could provide some theoretical basis for improving the stability of related products and constructing phage prevention and control measures, thereby reducing the losses caused by phage contamination in industrial production.

2. Materials and methods

2.1. Bacterial strain and culture conditions

The strain *L. fermentum* IMAU 32510 was isolated from the samples of traditional fermented yogurt collected from Ili Kazakh Autonomous Prefecture, Xinjiang Uygur Autonomous Region, China. It was stored at the Lactic Acid Bacteria Collection Center in Key Laboratory of Dairy Biotechnology and Engineering, Ministry of Education, Inner Mongolia Agricultural University, Hohhot, P.R. China. The bacterial strain was cultured at 37 °C in de Man, Rogosa, and Sharpe (MRS) broth for 24 h.

2.2. Phage induction

2.2.1. UV induction

The bacterial suspension ($OD_{600} \approx 0.5$) was irradiated by a 15 w UV lamp at five different time points: 40 s, 50 s, 60 s, 70 s and 80 s, positioned at a distance of 90 mm from the lamp. The inducing solution was then incubated at 37 °C for 6 h, during which the OD_{600} values were measured at hourly intervals (Kristin et al., 2021). Following, the inducing solution was centrifuged at 8000 g for 5 min and the supernatant was filtered through a 0.22 μm filter. Phage spots were examined using the double-layer agar (DLA) method (Stachurska et al., 2021).

2.2.2. MMC nduction

MMC was added into the bacterial suspension ($OD_{600} \approx 0.2$) to reach a final concentration of 1.8, 1.9, 2.0, 2.1, 2.2 μg/mL (Pei et al., 2020). The inducing solution was incubated at 37 °C for 6 h, in which the OD_{600} values were measured hourly. Then, the inducing solution was centrifuged at 8000 g for 5 min, the supernatant was filtered with 0.22 μm filters. The presence of phages in the supernatant was tested using DLA method.

2.3. Transmission electron microscopy (TEM)

A trace amount of phage lysate (ca. 10^8 PFU/mL) was taken and added dropwise on a copper grid, stained with 2% phosphotungstic acid (PTA, pH 7.0), and the morphology of the phage was observed using a HT7800 electron microscope (Hitachi High-Tech Corporation, Japan) at an acceleration voltage of 80 kV (Lu et al., 2020).

2.4. DNA extraction, whole genome sequencing and assembly

Phage DNA was extracted using the phenol-chloroform-isoamyl alcohol method (Boeckman et al., 2023). The details of the method were as follows: 2 mL SM buffer, 20 μL 10% SDS buffer, 2.5 μL 10 mg/mL Proteinase K, and 20 μL 0.5 M EDTA were added into the concentrated phage lysate. The mixture was then incubated at 65 °C for 15 min. Subsequently, an equal volume of phenol was added, and the mixture was centrifuged at 8000 g for 5 min. Next, an equal volume of phenol-chloroform-isoamyl alcohol (25:24:1) was added, and the mixture was centrifuged at 12,000 g for 5 min. The supernatant was transferred to a centrifuge tube. Then, an equal volume of chloroform was added for extraction until no odor of phenol remained. An equal volume of isopropanol was then added to the upper extraction solution, and the mixture was incubated at -20 °C for 30 min. Afterward, the mixture was centrifuged at 12,000 g for 20 min, and the precipitate was collected. The DNA precipitate was washed with 70% ethanol, centrifuged at 8000 g for 5 min, and the upper layer of ethanol was discarded. Finally, the precipitate was dried at room temperature for 5 -10 min, and 20 μL of distilled water was added to dissolve the precipitate. The sample was stored at - 20 °C.

The whole genome of the phage was sequenced by Anshan Biotechnology Co., Ltd. (Tianjin, China). The sequencing primarily utilized the PacBio Sequel sequencing platform with Sequel Binding Kit 2.0, Sequel Sequencing Kit 2.1 and Sequel SMRT Cell 1 M v2 (Pacific Biosciences, Menlo Park, CA, USA). Sequencing data was obtained for quality control. Then, the whole genome of the phage was assembled using Flye 2.8.3 (Kolmogorov et al., 2020).

2.5. Bioinformatic analysis

The ORF prediction was performed using Prodigal (https://github.com/hyattpd/Prodigal). The annotated coding sequences (CDS) of the phage genome were annotated using RAST (http://rast.nmpdr.org/). Subsequently, Proksee (https://proksee.ca/) was utilized to construct a genome map and visualize the position of functional proteins on the genome. A phylogenetic tree of different phages was constructed using the maximum likelihood method based on the terminase large subunit and major capsid protein, employing Molecular Evolutionary Genetics Analysis (MEGA, v7.0) software. The phylogenetic tree was then optimized and analyzed using iTOL (https://itol.embl.de/). Different phages in the phylogenetic tree were selected by BLAST (https://blast.ncbi.nlm.nih.gov/Blast.cgi) (Zhang et al., 2021; Kumar et al., 2016). The synteny analysis were implemented by MAUVE (https://asap.genetics.wisc.edu/) (Pillutla et al., 2021).

2.6. Phage host range

The DLA method was employed to assess the host range of the phage across 70 bacterial strains (Table A1), including *L. fermentum* (20 strains), *Lactobacillus helveticus* (10 strains), *Lactiplantibacillus plantarum* (10 strains), *Lactobacillus delbrueckii* subsp. *bulgaricus* (10 strains), *Lacticaseibacillus casei* (10 strains), *Limosilactobacillus reuteri* (10 strains). Specifically, 100 μL of phage lysate (ca. 10^8 PFU/mL) and 20 μL of various bacteria were separately added to semi-solid MRS medium. The mixture was then cultured overnight at 37 °C, and examined for the presence of phage plaque (Srikant et al., 2022).

Table 1
Functional grouping of annotated CDS in the phage LFP03 genome.

CDS	start	end	strand	Predicted function
CDS1	2	343	+	putative head-tail joining protein
CDS2	349	960	+	major tail protein
CDS4	1,568	5,860	+	tail tape measure protein
CDS6	6,728	8,809	+	tail tape measure protein
CDS11	14,392	15,516	+	baseplate
CDS45	36,585	37,196	+	head maturation protease
CDS46	37,214	38,335	+	capsid protein
CDS17	18,978	20,228	–	Mobile element protein
CDS18	20,302	20,757	+	Mobile element protein
CDS41	33,019	33,474	+	terminase small subunit
CDS42	33,471	35,180	+	terminase large subunit
CDS44	35,360	36,625	+	portal protein
CDS47	38,480	38,788	+	DNA packaging protein
CDS24	23,386	23,622	+	transcriptional regulator
CDS29	24,901	26,295	+	DNA helicase
CDS30	26,296	26,988	+	plasmid primase
CDS32	27,569	28,360	+	putative replication protein
CDS40	32,062	32,847	+	HNH endonuclease
CDS14	16,554	17,018	+	holin
CDS15	17,021	18,268	+	endolysin

"+" means on the positive strand and "-" means on the negative strand.

2.7. Optimal multiplicity of infection (MOI)

The MOIs were assessed by dividing the PFU by CFU (Benala et al., 2021). Phage and host bacterial suspension ($OD_{600} \approx 0.5$) were introduced into MRS broth with different MOI of 0.001, 0.01, 0.1, 0.5, 1, 2, 10, and 100, respectively. Subsequently, the mixture was incubated at 37 °C for 4 h, then filtered through 0.22 μm filters following centrifugation (8000 g, 5 min), and the phage titers were determined using the DLA method. The MOI with the highest phage titer was the optimal MOI.

2.8. One-step growth curve

Phage lysate and host bacteria were mixed based on the optimal MOI and allowed to adsorb at 37 °C for 15 min. Subsequently, the mixture was centrifuged (8000 g, 5 min) at 15 min intervals (0, 15, 30, 45, 60, 75, 90, 105, 120, 135 and 150 min). Samples from various time points were filtered and tested for titers using the DLA method. The one-step growth curve was plotted, and the latent and lysis periods of the phage were determined from the curve. The calculation formula for the burst size was shown below (Krasowska et al., 2015):

$$\text{Burst size} = N_1/N_0$$

Note: N_0: Bacteria amount at the initial infection (CFU); N_1: Phage amount at the end of the lysis period (PFU).

2.9. Influence of environmental factors on phage adsorption properties

2.9.1. Temperature

The phage and host bacteria were mixed at the optimal MOI. Subsequently, 200 μL of the mixture was added to 800 μL MRS broth. The mixture was then subjected different temperature conditions (0, 10, 20, 30, 37, 42 and 50 °C) for 30 min. After centrifugation (8000 g, 5 min), the supernatant was filtered through 0.22 μm filters, and the number of unadsorbed phages (N_1) in the supernatant was quantified using the DLA method. The phage adsorption rate was calculated as previously described (Sunthornthummas et al., 2017):

$$\text{Adsorption rate} = (N_0 - N_1)/N_0 \times 100\%$$

Note: N_0: The initial amount of phages(PFU); N_1: The amount of unadsorbed phages in the supernatant (PFU).

2.9.2. pH value

Phage lysate and host bacteria were mixed according to the optimal MOI. Subsequently, 200 μL mixture was added into 800 μL MRS broth at different pH values (4 - 10) and then incubated at 37 °C for 30 min. Following incubation, the mixture was centrifuged at 8000 g for 5 min, filtered through 0.22 μm filters, and the supernatant was collected and assessed for phage number (N_1) by DLA method. Then, the phage adsorption rate was calculated based on the formula described above.

2.9.3. Divalent cation

MRS-Ca and MRS-Mg broth were prepared at the final concentrations of 10 mM, and MRS broth was used as a control. Phage lysate (100 μL) and host bacteria (100 μL) were mixed according to the optimal MOI. The mixture was added into 800 μL of the above three different media, and was incubated at 37 °C. The sample was taken at 0, 15 and 30 min, respectively, then it was centrifuged at 8000 g for 5 min and filtered through 0.22 μm filters. The unadsorbed phage number (N_1) was counted by the DLA method to calculate the phage adsorption rate.

2.9.4. Chloramphenicol

The host bacteria ($OD_{600} \approx 0.5$) was centrifuged at 8000 g for 5 min. The resulting pellet was then resuspended in an equal volume of MRS broth, and 1 mL of the suspension was dispensed into a 2 mL Eppendorf tube. Chloramphenicol was added to achieve final concentrations of 20 and 100 μg/mL, while the MRS broth without chloramphenicol served as the control. Following an incubation period at 37 °C for 75 min, 100 μL phage lysate was added according to the optimal MOI. The mixture was then incubated at 37 °C for an additional 30 min. After incubation, the mixture underwent centrifugation at 8000*g* for 5 min and was subsequently filtered through 0.22 μm filters. The number of unadsorbed phages (N_1) was determined using the DLA method, enabling the calculation of the phage adsorption rate.

2.10. Environmental factors influencing phage viablity

2.10.1. Temperature

Mixed 900 μL MRS broth with 100 μL phage lysate, then incubated the mixture at various environmental temperatures (0, 10, 20, 30, 37, 42 and 50 °C) for 30 min. Following the incubation, the phage titer (N_1) was counted by using the DLA method, the survival rate was then calculated by using the following fomula (Abedon, 2023):

$$\text{Survival rate} = N_1/N_0 \times 100\%$$

Note: N_0: Phage initial titer (PFU/mL); N_1: Phage titer after treatment (PFU/mL).

2.10.2. pH value

Mixed 900 μL MRS broth with different pH values (2 - 11) into 100 μL of phage lysate, respectively. Then, incubated the tubes at 37 °C for 30 min. After incubation, the phage titer (N_1) was counted by using the DLA method for calculating the phage survival rate.

2.11. Statistical analysis

All data were analyzed using Microsoft Excel 2019. The above experiments had been verified by three repeated experiments. Means were compared using a one-way ANOVA by SPSS 20.0 software (SPSS Inc, Chicago, IL, USA).

3. Results

3.1. Phage induction

UV and MMC treatments are commonly employed to induce prophages. The results of UV and MMC induction are shown in Fig. 1. As shown in Fig. 1a, the OD_{600} values of the induced solutions after UV irradiation were all lower than the control group, with the lowest OD_{600} value of 0.57 at 70 s treatment. From Fig. 1b, we can find the OD_{600} values of the induced solution after MMC induction were lower than the control group. The higher the MMC concentration, the lower the OD_{600} value. The lowest OD_{600} value was 0.73 when the MMC concentration was 2.5 μg/mL.

The induced solutions under different conditions were examined by the DLA method. Phage plaque was proved to be present after 70 s of UV irradiation (Fig. 2), and the induced phage was named LFP03. However, there was no phage plaque appeared in any of the other experimental groups.

3.2. Transmission electron microscopy

The electron microscopy (Fig. 3) showed that phage LFP03 had an isometric capsid of 68.53 ± 2.46 nm, and a non-contractile tail (232.76 ± 2.92 nm long and 11.02 ± 1.51 nm wide). According to the latest classification guidelines proposed by the International Committee on Taxonomy of Viruses (ICTV), phage LFP03 belonged to the *Caudoviricetes* class.

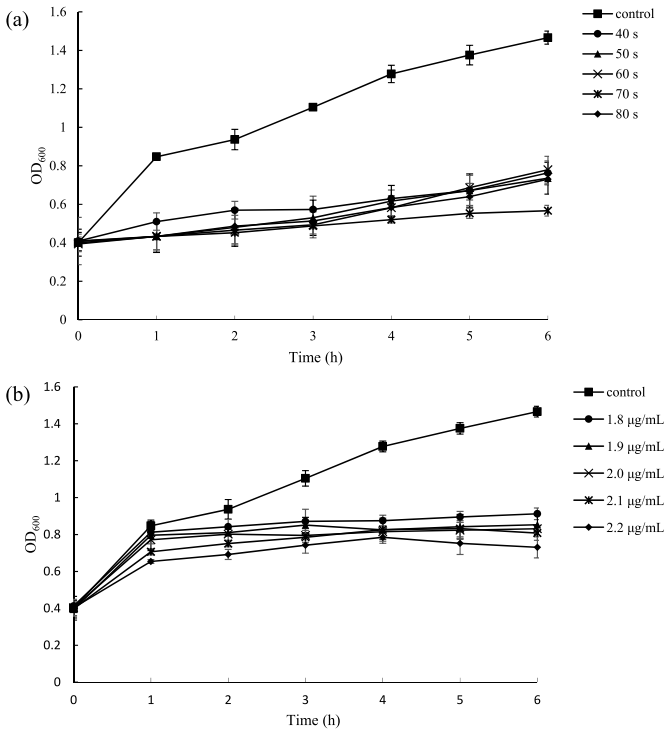

Fig. 1. The changes in OD_{600} value of *L. fermentum* IMAU 32510 during induction: (a) UV induction; (b) MMC induction. Values were the means of three determinations.

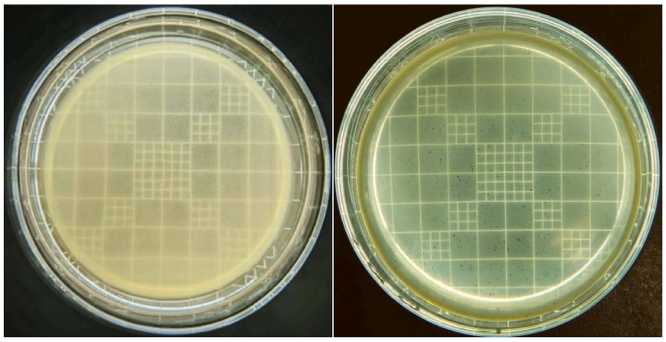

Fig. 2. Morphological observation of phage plaque. The left is a control plate and the right is the plate after 70 s of UV irradiation.

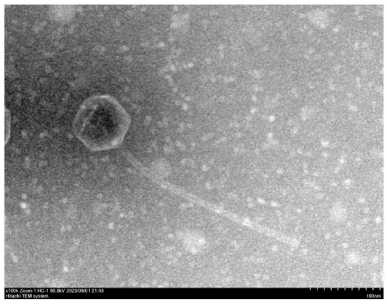

Fig. 3. Electron microscope of *L. fermentum* phage LFP03.

3.3. Genome sequence analysis of phage LFP03

The whole genome sequencing results revealed that phage LFP03 contained a linear double-stranded DNA (Fig. 4). Its genome size was 39,556 bp and the GC content was 46.08%. The genome was annotated to 223 ORFs and 48 CDS, of which 20 CDS were annotated specific functions. As shown in Table 1, the annotated functions fall into four main categories: structural proteins, DNA packaging, DNA replication, and host lysis. Interestingly, the presence of plasmid primase (CDS30) but not integrase in phage LFP03 demonstrates that the phage is presented in the host cell precisely in the form of plasmid (Shan et al., 2023).

3.4. Comparative genomic analysis

Phylogenetic tree analysis basedon bacterial 16S rRNA sequence (Fig. 5 a) showed that IMAU 32510 was closest to the other two *L. fermentum* strains, therefore IMAU 32510 could be identified as *L. fermentum* strain. In Fig. 5 (b) and (c), the phylogenetic tree showed that the evolutionary distance of phage LFP03 was more closely related to phage LFP02, LF1 and phiPYB5. Previous studies had shown that *L. fermentum* phage LFP02, LF1 and phage phiPYB5 were lysogenic phages, and their host strains were isolated from yogurt, kimchi and yogurt, respectively (Lv et al., 2023a; Yoon and Chang, 2011; Wang et al., 2008), which were similar with the source of the host strain of phage LFP03 (traditional fermented yogurt). However, the host strains of *L. fermentum* lysogenic phage JNU_P1 and JNU_P5 were isolated from human feces, which were different from the isolation source of IMAU32510, and thus there was a large genetic distance (Pei et al., 2020). As for *L. fermentum* virulent phage LfeInf (which was isolated from waste water), its infestation characteristics were different from those of lysogenic phage LFP03, and its isolation source differed significantly from that of the host strain of phage LFP03, thus the branches were widely separated (Liu et al., 2015).

This study further revealed the relationship between the genome of phage LFP03 and other closely related phages through synteny analysis. As shown in Fig. 6, high similarity fragments were marked with the same color and linked. Compared with other phages, phage LFP03 genome had obvious deletions, inversions and translocations, and its genome contained about 18.8 Kb of specific gene fragments. Based on the above genomic analysis, it could be indicated that phage LFP03 was a novel phage.

3.5. Phage host range

In this study, 70 LAB strains were used for the host range experiment (Table A1). The results showed that phage LFP03 could infect *L. fermentum* IMAU32579, IMAU32646, IMAU32649 and IMAU32229. All of the above four strains were isolated from traditional fermented yogurt in Yili Kazakh Autonomous Prefecture, Xinjiang, which was same as the host strain IMAU32510 of phage LFP03. However, phage LFP03 could not infect other bacterial strains.

3.6. Determination of the optimal MOI

The phage titers under different MOI were counted using DLA method, and the results were shown in Fig. 7. When MOI <0.1, the phage titer gradually decreased as MOI decreased. When MOI >0.1, the phage titer gradually decreased as MOI increased. At the MOI of 0.1, the phage had a maximum titer of 1.9×10^9 PFU/mL, thus the optimal MOI of phage LFP03 was 0.1.

3.7. One-step growth curve

As shown in Fig. 8, the number of the phage was low and almost unchanged in 0–30 min; it entered the lysis period and grew rapidly in 30–75 min; after 75 min, it increased but generally stabilized. From the one-step growth curve, it could be seen that the latent period of phage LFP03 was 30 min, the lysis period was 45 min, and the burst size was 133.5 ± 4.9 PFU/infective cell.

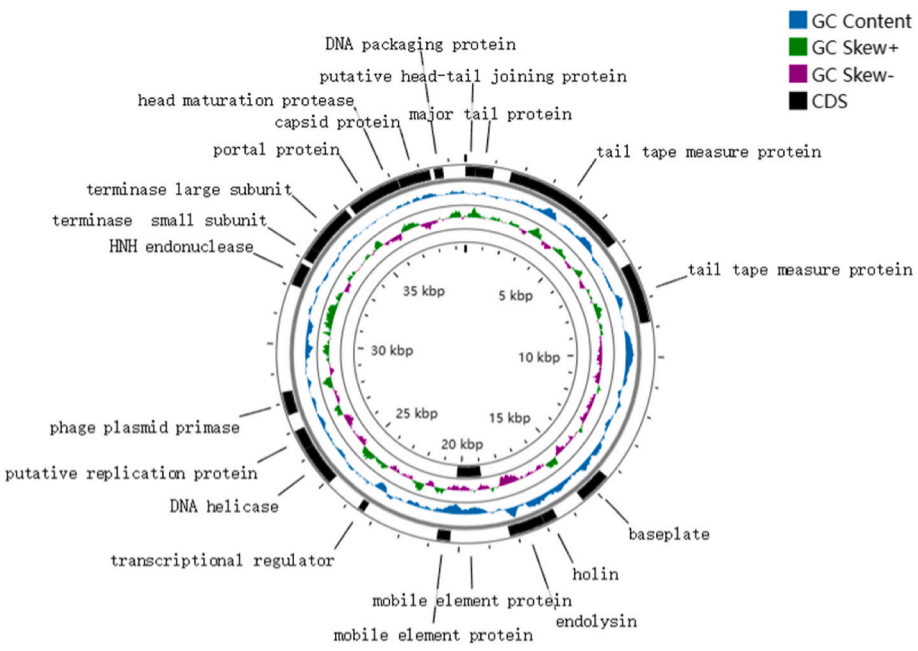

Fig. 4. Circular genome map of *L. fermentum* phage LFP03. The innermost circle of the genome map showed the genome size, the second circle was the GC backbone on the positive and negative strands, the third circle represents the GC content, and the outermost circle represents each CDS.

3.8. Influence of environmental factors on phage adsorption properties

3.8.1. Temperature

As shown in Table 2, in the range of 0–37 °C, the adsorption rates of phage LFP03 rose with the increase of temperature, and the highest was 99.43% at 37 °C. However, the adsorption rates decreased when the temperature was higher than 37 °C, but still was 81.21% even at 50 °C.

3.8.2. pH value

As for the effect of different pH values on the adsorption rate of phage LFP03 (Table 3), the highest adsorption rate of phage was 99.07% at pH 7. The adsorption rates were higher than 85% at different pH values, but reduced when in acidic or alkaline environment, and reached the minimum adsorption rate of 88.06% at pH 4.

3.8.3. Divalent cation

The adsorption rates of phage LFP03 could reach over 90% in all three media within 15 min (Table 4). The adsorption rates in MRS-Ca and MRS-Mg broth were significantly higher than those in MRS broth at 15 min. However, by 30 min, there was no significant difference in the adsorption rates of phage LFP03 among the three media.

3.8.4. Chloramphenicol

There was no significant difference in the phage adsorption rate between the medium containing or without chloramphenicol, and adsorption rates were all higher than 90% (Table 5). As the concentration of chloramphenicol increased, the adsorption rates of phage LFP03 did not change significantly, proving that chloramphenicol had no effect on phage adsorption.

3.9. Influence of environmental factors on phage viability

3.9.1. Temperature

As shown in Fig. 9, the phage survival rates were significantly affected by temperature changes ($P < 0.05$). The survival rates of phage LFP03 rose with the increase of temperature from 0 to 37 °C, and the highest survival rate was 93.06% at 37 °C. When the temperature was higher than 37 °C, the survival rate decreased significantly, and the lowest survival rate was 48.98% at 50 °C.

3.9.2. pH value

According to Fig. 10, the survival rates of phage LFP03 were significantly affected by pH value ($P < 0.05$). Under low or high pH conditions, the survival rates decreased significantly. Phage LFP03 was completely inactivated at pH 2, and the survival rate was only 3.95% at pH 3. When pH was 7, the survival rate of phage LFP03 reached the highest (97.60%). With the increase of pH value, the survival rates began to decrease again. When pH was 11, the survival rate of phage was 38.32%. The tolerance to acidic and alkaline environment was low, which may be related to the structure of phage.

4. Discussion

Phage contamination is a major challenge jeopardizing industrial fermentation production (Li et al., 2019). The starter culture is a screened LAB population, however, some of them may in relatively phage-sensitive (Hayes et al., 2017). Prophage genes are widely presented in bacteria and replicate along with the host cells. When stimulated by external conditions, prophage genes may be activated into lytic cycle and lyse host cells. Once phage contamination occurs, a large number of starter cultures will die, and thus fermentation will be delayed or stopped, resulting in serious economic losses (Kubo et al., 2018). Although there are many methods to inactivate phages in industrial production, it is difficult to control phage once it is contaminated. Therefore, a study on the biological and genomic characteristics of phage can help to understand the mechanism of phage infestation and reduce the possibility of phage infestation from the source.

UV and MMC are commonly used to induce phages in the laboratory. Zhang et al. (2020) induced 8 *Escherichia coli* strains under a variety of conditions and found that UV could successfully induce phages. Feyereiseni et al. (2019) performed MMC induction on 19 *Lactobacillus brevis* strains and obtained five lysogenic phages. Köppen et al. (2021) conducted UV and MMC induction on *Francisella hispaniensis* and obtained lysogenic phage vB_FhiM_KIRK by UV irradiation for 60 s and 90 s. Similar to the previous studies, phage LFP03 was induced from *L. fermentum* by UV irradiation. Some previous studies have shown that UV irradiation can make bacteria produce a variety of reactive oxygen species (ROS). The strong oxidation ability of ROS can damage biological macromolecules such as DNA and proteins of bacteria, thus

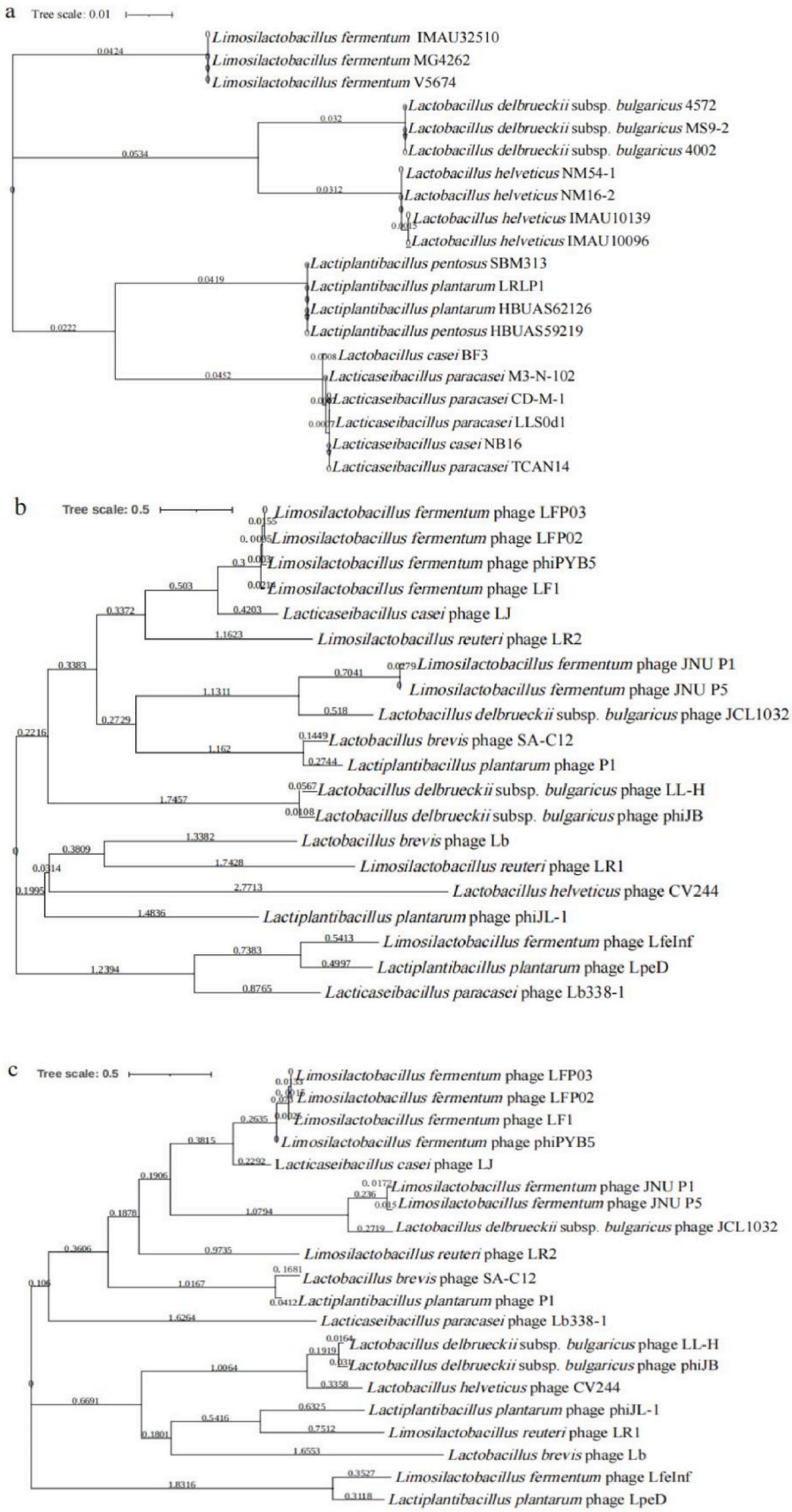

Fig. 5. Phylogenetic trees of bacteria and phages. (a) Phylogenetic tree constructed based on the 16S rRNA sequences of bacteria. Phylogenetic analysis of (b) major capsid protein and (c) terminase large subunit in *Lactobacillus* phages by Maximum-Likelihood method.

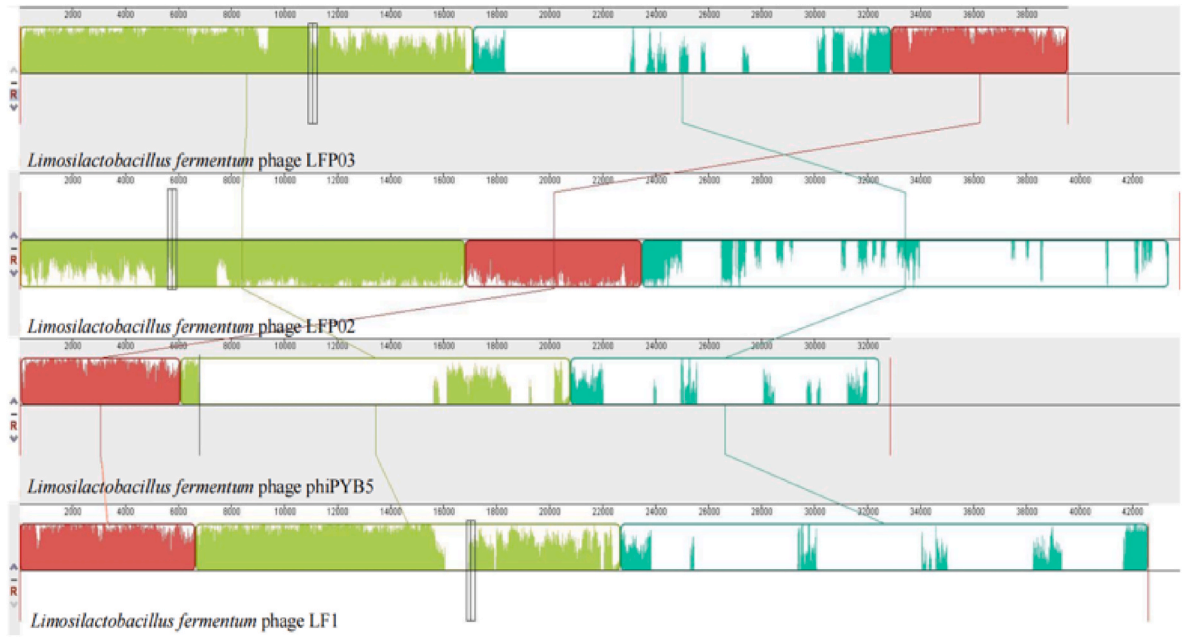

Fig. 6. Synteny analysis of *L. fermentum* phage LFP03, LFP02, LF1 and phiPYB5.

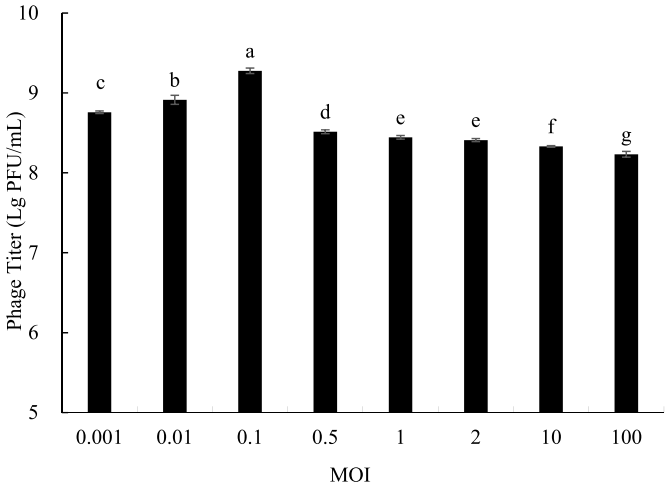

Fig. 7. The multiplicity of infection of phage LFP03. Different lowercase letters represented significant differences in phage titer ($P < 0.05$). Values were the means of three determinations.

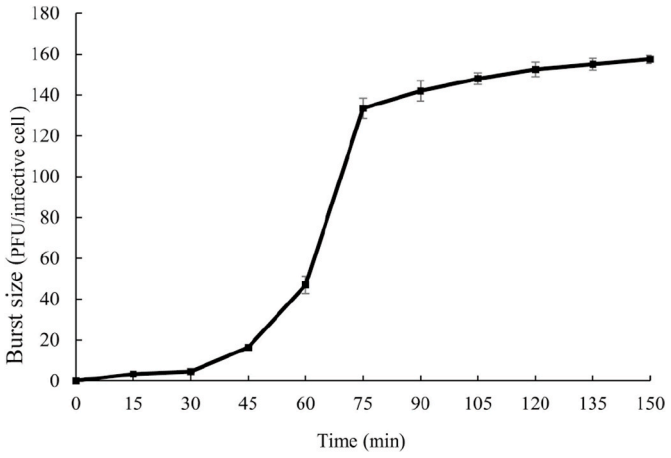

Fig. 8. One-step growth curve of *L. fermentum* phage LFP03. Values were the means of three determinations.

triggering SOS reaction and eventually leading to phage induction (Kieft and Anantharaman, 2022; Kondo et al., 2021;Wang et al., 2022). During phage induction, transcriptional regulator (CDS24) is activated, allowing lysogenic phage to enter the lysis cycle. DNA helicase (CDS29), replication protein (CDS32) and HNH endonuclease (CDS40) are essential for the synthesis of phage DNA in subsequent processes (Howard-Varona et al., 2017).

Phage particle formation requires the interaction of various proteins within the phage. Phage packaging is divided into three main parts and mobile element proteins play a function in which they transport DNA fragments in the genome (Sun et al., 2012). The first part is the portal protein (CDS44), which is located at the special fivefold vertex of the capsid and is a key component of the DNA packaging. The second part is the terminase small subunit (CDS41), which recognizes and binds to phage DNA and is the part of initiating packaging. The third part is the terminase large subunit (CDS42), which has nuclease activity for packaging initiation and cleaves phage DNA (Chen et al., 2020). Terminase large subunit and capsid protein are often considered as conserved regions in the phage genome thus they are widely used to study evolutionary relationships (Zhang et al., 2021).

Table 2
Adsorption rates of phage LFP03 under different temperatures.

Temperature (°C)	Adsorption Rate (%)
0	88.61 ± 0.57^{f}
10	91.73 ± 0.90^{e}
20	94.57 ± 1.16^{c}
30	98.12 ± 0.49^{b}
37	99.43 ± 0.22^{a}
42	93.93 ± 0.25^{d}
50	81.21 ± 0.65^{g}

The significant differences ($P < 0.05$) among the groups were expressed by different lowercase letters.

Lysogenic phages can exist as plasmid in host cells without being integrated in their chromosomes (Shan et al., 2023). The presence of plasmid primase (CDS30) but not integrase in phage LFP03

Table 3
Adsorption rates of phage LFP03 under different pH values.

pH	Adsorption Rate (%)
4	88.06 ± 0.39^{g}
5	92.35 ± 0.14^{e}
6	98.49 ± 0.18^{b}
7	99.07 ± 0.10^{a}
8	95.68 ± 0.06^{c}
9	93.21 ± 1.02^{d}
10	90.00 ± 0.57^{f}

The significant differences ($P < 0.05$) among the groups were expressed by different lowercase letters.

Table 4
Adsorption rates of phage LFP03 under different medium containing divalent cations.

Medium/Time (min)	Adsorption rate (%)		
	0	15	30
MRS	0	93.57 ± 0.71^{b}	98.22 ± 0.94^{a}
MRS-Ca	0	96.67 ± 1.25^{a}	99.48 ± 1.66^{a}
MRS-Mg	0	96.48 ± 1.33^{a}	98.97 ± 1.09^{a}

The significant differences ($P < 0.05$) among the groups were expressed by different lowercase letters.

Table 5
Adsorption rates of phage LFP03 under MRS medium containing the different conentrations of chloramphenicol.

Concentrations (μg/mL)	Adsorption rate (%)
0	98.44 ± 1.05^{a}
20	98.97 ± 0.74^{a}
100	98.76 ± 1.76^{a}

The significant differences ($P < 0.05$) among the groups were expressed by different lowercase letters.

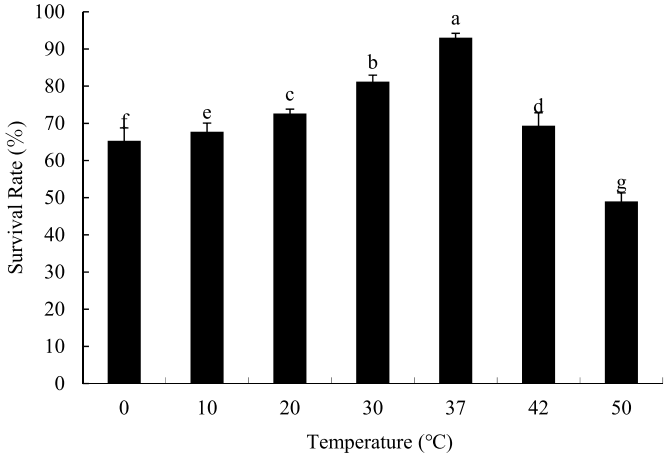

Fig. 9. Survival rates of phage LFP03 under different temperature conditions. The significant differences ($P < 0.05$) among the groups were expressed by different lowercase letter, and values were the means of three determinations.

demonstrates that the phage is presented in the host cell precisely in the form of a plasmid. The head-tail joining protein (CDS1) plays an important role in the assembly process of long-tailed double-stranded DNA phage particles by facilitating the attachment of the head to the tail (Cardarelli et al., 2010). The tube of phage tails is composed primarily of multiple copies of one protein, known as the major tail protein (CDS2)

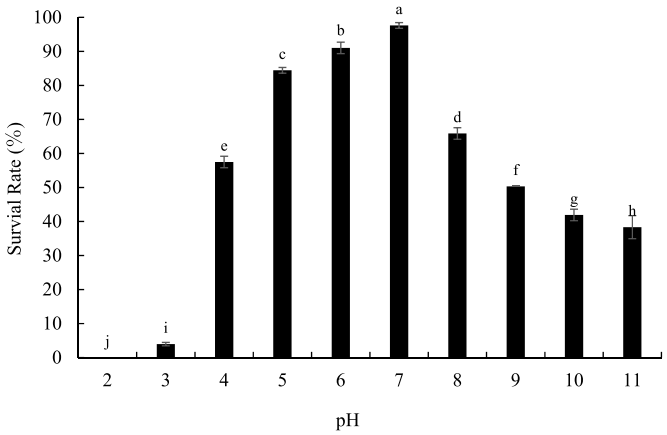

Fig. 10. Survival rates of phage LFP03 under different pH values. The significant differences ($P < 0.05$) among the groups were expressed by different lowercase letter and values were the means of three determinations.

(Pell et al., 2009). Baseplate (CDS11) and tail tape measure protein (CDS4 and CDS6) are often considered to play an important role in phage adsorption and infestation (Linares et al., 2020). Head maturation protease (CDS45) destroys the interior of the capsid protein (CDS46) as it forms, providing storage space for the genetic material (Fokine and Rossmann, 2016).

Using the genome sequences of terminase large subunit and major capsid protein to construct a phylogenetic tree enables a better understanding of the evolutionary relationships among different phage sequences (Al-Shayeb et al., 2020). Zhu et al. (2022) constructed a phylogenetic tree by combining *Lactiplantibacillus plantarum* phage P2 with 19 other *Lactiplantibacillus plantarum* phage sequences obtained from the NCBI database, and found that the phages whose host bacteria isolated from the same isolation source were clustered to the same branch. Hyde et al. (2024) constructed a phylogenetic tree of 103 phage genome sequences of terminase large subunit by using maximum likelinood method, and found that the phages isolated from the same bacterial genera clustered in a same branch. In this study, phage LFP03 was found to be in the same branch as three other lysogenic *L. fermentum* phages (phage LFP02, LF1 and phiPYB5), and all of their host bacteria were isolated from traditional fermented products. Therefore, phages that are isolated from the same bacterial genus and from similar host isolation sources tend to display a closer evolutionary relationship at the genomic level.

Phage infection is an important factor threatening the fermentation industry. The genetic material of phage increases with the replication of the host bacterial genetic material, but assembly is not completed and phage cannot be produced, hence this period is called the latent period (Zaburlin et al., 2017). As the phage is released, it represents entering the lysis period and eventually stabilized (Chaturongakul and Ounjai, 2014). MOI represents the number of phages that infect a cell. Different phages have different MOI, and larger MOI represent a weaker infective ability (Zhang et al., 2021). Zhang et al. (2015) found the *Lactobacillus casei* phage LAB had an MOI of 0.1, its latent period was 75 min and burst size was 16 PFU/infective cell, and it only infected its host strain. Sunthornthummas et al. (2017) obtained a lysogenic phage ΦT25 from *Lactobacillus paracasei*, and found it was only able to infect its host strain. Its one-step growth curve showed that the latent period was 55 min and the burst size was about 38 PFU/infected cell. Zago et al. (2015) performed a one-step growth curve study on 6 *Lactobacillus helveticus* phages according to an MOI of 2, and found that one phage had a minimum latent period of 53 min, whereas the other five strains had latent periods longer than 99 min and two of the phages (ΦAQ113, ΦAQ114) with burst size of around 90 PFU/infective cell. Compared to above *Lactobacillus* phages, phage LFP03 had a smaller MOI (0.1),

proving a greater infestation ability. Phage LFP03 had a shorter latent period (30 min) and larger burst size (133.5 ± 4.9 PFU/infective cell). A short latent period means that the host bacteria can be lysed in a shorter time after adsorption; a large burst size means that more phages are prepared (Ye et al., 2022). In this study, only four strains of *L. fermentum* can be infected by LFP03 phage. In the process of phage infection, phage specifically recognizes and binds to the surface receptors of host cells, and then passes through the barriers such as cell walls and cell membranes, so as to inject its own genetic material into the cytoplasm and then complete the infection. (Zampara et al., 2020). Thus, the reason that phage LFP03 lyses the other four bacteria may be that the viral proteins called receptor binding proteins (RBP) recognizes host bacteria of similar isolation source (traditional fermented yogurt) and similar isolation location (Yili Kazakh Autonomous Prefecture, Xinjiang), which undergoes irreversible binding and thus continues to complete the process of infection, leading to the lysis of the four strains (Dunne et al., 2019). During phage lysis of cells, holin (CDS14) and endolysin (CDS15) are particularly important. Holin permeabilizes the inner membrane of the host cell, allowing endolysin to enter and degrade cell wall peptidoglycan (Oechslin et al., 2022). With the cooperative action of the two proteins, the phage completes the lysis of the host cell, leading to its destruction.

Adsorption is a particularly important step in the process of phage infection. Phage adsorption to host bacteria depends on specific recognition and receptors on the surface of the host bacteria (Leprince and Mahillon, 2023). The phage encounters the host bacteria through diffusion and Brownian motion at first, then the RBP bind reversibly to receptors on the surface of the host bacteria, during which they may separate to later bind to other receptors and eventually irreversibly bind and inject their genetic material into the host bacteria (Thanki et al., 2018; Silva et al., 2016). The genome annotation results showed that phage LFP03 held a baseplate (CDS11) which contained RBP that specifically recognized host bacteria surface receptors to accomplish adsorption (Bebeacua et al., 2010). Upon irreversible binding, the tail tape measure proteins (CDS4, CDS6) can undergo a conformational change that results in the ejection of phage DNA into the cytoplasm within the host bacterium (Mahony et al., 2016).

The adsorption process is susceptible to a multitude of physical or chemical factors in the environment, such as temperature, pH value, divalent cations, antibiotics, etc (Jeon and Ahn, 2020; Pujato et al., 2015). Li et al. (2020) revealed that *Bacillus cereus* phage vB_BceP-DLc1 had a temperature-dependent adsorption ability, and the highest adsorption rate was 85% at 37 °C. Mercanti et al. (2015) detected the adsorption ability of *Lactobacillus paracasei* phages ΦiLp84 and ΦiLp1308, and found that the adsorption rates were highest at 37 °C. The adsorption abilities of these two phages were more stable in pH 5–8. While they were inhibited at pH 4 or 9. The adsorption rates of phage LFP03 was higher than 80% at all temperatures and pH conditions, which proved that the adsorption ability of phage LFP03 was less influenced by the temperature and pH in the environment. The temperature changes could affect the structure of RBP on the phage surface, which in turn has an effect on phage adsorption. In addition, different pH values may cause changes in the adsorption sites or receptor charges on the surfaces of the host bacterium and phage, which may have an effect on the electrostatic interaction between them (Echeverría-Vega et al., 2020).

At the same time, the influence of divalent cations on the phage adsorption process had also been studied. Ullah et al. (2017) analyzed the effects of Ca^{2+} and Mg^{2+} on the adsorption rate of *Enterococcus faecalis* phage SRG1. The results demonstrated that the adsorption rate of phage SRG1 was increased when the concentrations of Ca^{2+} and Mg^{2+} were 10 mM, respectively, indicating that divalent cations could enhance the adsorption effect. Trucco et al. (2011) found that the presence of Ca^{2+} could greatly increase the adsorption rate of *Lactobacillus delbrueckii* phage Cb1/342. Chen et al. (2019) found that divalent cations had no significant effect on the adsorption properties of *Lactobacillus plantarum* P2. The effect of divalent cations on the adsorption process was different for different phages. In this study, the adsorption rates of phage LFP03 could be significantly increased in the medium containing divalent cations at 15 min, indicating that divalent cations could accelerate the adsorption of phage LFP03, but the adsorption rates were not significantly different among the three media at 30 min. The cause for the acceleration of phage adsorption was mainly due to the host bacterial cell receptor and phage RBP tend to be negatively charged, so it was possible to make phage adsorption on the cell surface by electrostatic force of gravity through the addition of divalent cations (Yuan et al., 2022).

Chloramphenicol treatment can lead to the inhibition of cellular protein synthesis and a decrease in the amount of membrane proteins synthesized by the bacteria, which leads to a decrease in the amount of RBP recognized by the phage, and thus affects phage adsorption to some certain extent (Jeon and Ahn., 2021). Lv et al. (2023b) found that after 45 min of culture, the adsorption rate of *Bacillus methylotrophicus* phage BM-P1 did not change regardless of the presence or absence of chloramphenicol. Which showed that antibiotics have no effect on adsorption ability. Similar to the above finding, chloramphenicol had no effect on the adsorption rate of phage LFP03.

Environment changes, such as temperature and pH value, may cause changes in phage resistance. Thus, phage tolerance study can provide some theoretical support for the inactivation and control of phage in industrial production (Xu et al., 2023). Hu et al. (2021) conducted an environmental tolerance study and found that phage PH669 was temperature and pH stable, with the survival rates were all higher than 80% at 4–37 °C and pH 3–10. Gao et al. (2023) found that the phage titers of *Salmonella* phage GSP044 were essentially unchanged at temperatures of 4–60 °C. When at pH 3–11, the phage titers decreased but did not vary significantly. Huang et al. (2022) conducted tolerance study on phage vB_CpeS_BG3P and found that the phage was highly tolerant, even survived at pH 2 and 12, and the phage titer remained almost unchanged (<0.5 log) after treatment at 50 °C for 30 min. Compared with the phages studied above, phage LFP03 was poorly tolerant to the change of temperature and pH value. The survival rates were lower than 80% at all temperatures except 30 and 37 °C. It was sensitive to pH value, the survival rates were only 3.95% and 38.32% at pH 3 and 11. The reason may be that temperature and pH value influence phage viability by destroying the spatial structure of proteins and inhibiting enzyme activity (Abedon, 2023). When the temperature is lower than the optimal temperature, the enzyme activity is inhibited and the physiological activity is reduced; when exposed to higher temperatures, microorganisms are unable to normally carry out their biological activities because the structure of their nucleic acids, proteins and other biomolecules are destroyed. As for pH tolerance, the activity of proteins and other macromolecules within the phage is inhibited when not in optimal pH conditions, thus reducing phage tolerance (Fontanal et al., 2019).

5. Conclusion

In this study, a novel lysogenic phage LFP03 was obtained by UV induction from *L. fermentum*, and its biological properties and genome information was investigated. Phage LFP03 belonged to the *Caudoviricetes* class. Its genome size was 39,556 bp and the GC content was 46.08%. Compared with other *L. fermentum* phages, the genome of phage LFP03 had deletions, inversions and translocations. Phage adsorption rates were affected by temperature and pH value, but were above 80% in all cases. Divalent cations (Ca^{2+}, Mg^{2+}) could accelerate phage adsorption, but chloramphenicol expressed little effect on the adsorption of phage LFP03. Phage LFP03 was poorly tolerant to temperature and pH value, with a minimum survival rate of 48.98% at 50 °C and could be completely inactivated at pH 2. This study could expand the study of genomic information and biological characteristics of *L. fermentum* phages, and provid some theoretical basis for phage control and screening of phage resistant strains.

Ethics approval and consent to participate

This article does not contain any studies involving humans or animals.

Consent for publication

Not applicable.

Availability of data and materials

The data that support the findings of this study are available from the corresponding author upon reasonable request.

Competing interests

The authors have no competing interests to declare that are relevant to the content of this article.

Funding

This work was supported by Central-directed Local Projects, China (Grant No. 2021ZY0022), Natural Science Foundation of China (Grant No. 32160550), Natural Science Foundation of Inner Mongolia, China (Grant No. 2021MS03014), Higher Education Reform and Development Program, China (Grant No. DC2300002880), Inner Mongolia Science & Technology Plan, China (Grant No. 2021GG0080).

Credit Author Statement

Conceptualization: [Can Zhang, Xingyu Quan, Xia Chen], Methodology: [Can Zhang, Xingyu Quan, Xia Chen], Formal analysis and investigation: [Can Zhang, Xingyu Quan, Weiqi Lian, Runze Liu and Qiannan Wen], Writing – original draft preparation: [Can Zhang, Xingyu Quan,]; Funding acquisition: [Xia Chen], Supervision: [Xia Chen].

Declaration of competing interest

The authors declare that they have no known competing financial interests or personal relationships that could have appeared to influence the work reported in this paper.

Data availability

Data will be made available on request.

Appendix A. Supplementary data

Supplementary data to this article can be found online at https://doi.org/10.1016/j.crfs.2024.100748.

References

Abedon, S.T., 2023. Ecology and evolutionary biology of hindering phage therapy: the phage tolerance vs. phage resistance of bacterial biofilms. Antibiotics 12, 245. https://doi.org/10.3390/antibiotics12020245.

Al-Shayeb, B., Sachdeva, R., Chen, L.X., Ward, F., Munk, P., Devoto, A., Castelle, C.J., Olm, M.R., Bouma-Gregson, K., Amano, Y., He, C., 2020. Clades of huge phages from across Earth's ecosystems. Nature 578, 425–431. https://doi.org/10.1038/s41586-020-2007-4.

Bebeacua, C., Bron, P., Lai, L., Vegge, C.S., Brøndsted, L., Spinelli, S., Cambillau, C., Veesler, D., Heel, M.V., Cambillau, C., 2010. Structure and molecular assignment of *Lactococcal* phage TP901-1 baseplate. J. Biol. Chem. 285, 39079–39086. https://doi.org/10.1074/jbc.M110.175646.

Benala, M., Vaiyapuri, M., Visnuvinayagam, S., George, J.C., Raveendran, K., George, I., Mothadaka, M.P., Badireddy, M.R., 2021. A revisited two-step microtiter plate assay: optimization of in vitro multiplicity of infection (MOI) for Coliphage and Vibriophage. J. Virol Methods 294, 114177. https://doi.org/10.1016/j.jviromet.2021.114177.

Cantu, V.A., Salamon, P., Seguritan, V., Redfield, J., Salamon, D., Edwards, R.A., Segall, A.M., 2020. PhANNs, a fast and accurate tool and web server to classify phage structural proteins. PLoS Comput. Biol. 16, e1007845 https://doi.org/10.1371/journal.pcbi.1007845.

Cardarelli, L., Lam, R., Tuite, A., Baker, L.A., Sadowski, P.D., Radford, D.R., Rubinstein, J.L., Battaile, K.P., Chirgadze, N., Maxwell, K.L., Davidson, A.R., 2010. The crystal structure of bacteriophage HK97 gp6: defining a large family of head-tail connector proteins. J. Mol. Biol. 395, 754–768. https://doi.org/10.1016/j.jmb.2009.10.067.

Chaturongakul, S., Ounjai, P., 2014. Phage-host interplay: examples from tailed phages and Gram-negative bacterial pathogens. Front. Microbiol. 5, 442. https://doi.org/10.3389/fmicb.2014.00442.

Chen, W.Y., Xiao, H., Wang, X.R., Song, S.L., Han, Z., Li, X.W., Yang, F., Wang, L., Song, J.D., Liu, H.R., Cheng, L.P., 2020. Structural changes of a bacteriophage upon DNA packaging and maturation. Protein Cell 11, 374–379. https://doi.org/10.1007/s13238-020-00715-9.

Chen, X., Guo, J., Liu, Y., Chai, S.Y., Ma, R.R., Munguntsetseg, B., 2019. Characterization and adsorption of a *Lactobacillus plantarum* virulent phage. J. Dairy Sci. 102, 3879–3886. https://doi.org/10.3168/jds.2018-16019.

Dunne, M., Rupf, B., Tala, M., Qabrati, X., Ernst, P., Shen, Y., Sumrall, E., Heeb, L., Plückthun, A., Loessner, M.J., Kilcher, S., 2019. Reprogramming bacteriophage host range through structure-guided design of chimeric receptor binding proteins. Cell Rep. 29, 1336–1350. https://doi.org/10.1016/j.celrep.2019.09.062.

Echeverría-Vega, A., Morales-Vicencio, P., Saez-Saavedra, C., Alvarez, M.A., Gordillo, F., Del-Valle, R., Solís, M.E., Araya, R., 2020. Characterization of the bacteriophage vB_VorS-PVo5 infection on *Vibrio Ordalii*: a model for phage-bacteria adsorption in aquatic environments. Front. Microbiol. 11, 550979 https://doi.org/10.3389/fmicb.2020.550979.

Ephrem, E., Najjar, A., Charcosset, C., Greige-Gerges, H., 2019. Selection of nerolidol among a series of terpenic and phenolic compounds for its potent activity against *Lactobacillus fermentum* ATCC 9338. Process Biochem. 80, 146–156. https://doi.org/10.1016/j.procbio.2019.02.015.

Feyereiseni, M., Mahony, J., Neve, H., Franz, C.M.A.P., Noben, J.P., Sullivan, T.O., Boer, V., Sinderen, D.V., 2019. Biodiversity and classification of phages infecting *Lactobacillus brevis*. Front. Microbiol. 10, 2396. https://doi.org/10.3389/fmicb.2019.02396.

Fokine, A., Rossmann, M.G. Common evolutionary origin of procapsid proteases, phage tail tubes, and tubes of bacterial type VI secretion systems. Structure 24, 1928-1935. https://doi.org/10.1016/j.str.2016.08.013..

Fontanal, A., Falasconi, I., Molinaril, P., Treu, L., Basile, A., Vezzi, A., Campanaro, S., Morelli, L., 2019. Genomic comparison of *Lactobacillus helveticus* strains highlights probiotic potential. Front. Microbiol. 10, 1380. https://doi.org/10.3389/fmicb.2019.01380.

Gao, D.Y., Ji, H.Y., Li, X., Ke, X.Q., Li, X.M., Chen, P., Qian, P., 2023. Host receptor identification of a polyvalent lytic phage GSP044, and preliminary assessment of its efficacy in the clearance of *Salmonella*. Microbiol. Res. 273, 127412 https://doi.org/10.1016/j.micres.2023.127412.

Hayes, S., Murphy, J., Mahony, M., Lugli, G.A., Ventura, M., Noben, J.P., Franz, C.M.A.P., Neve, H., Nauta, A., Sinderen, D.V., 2017. Biocidal Inactivation of *Lactococcus lactis* bacteriophages: efficacy and targets of commonly used sanitizers. Food Microbiol. 8, e00107 https://doi.org/10.3389/fmicb.2017.00107.

Howard-Varona, C., Hargreaves, K.R., Abedon, S.T., Sullivan, M.B., 2017. Lysogeny in nature: mechanisms, impact and ecology of temperate phages. ISME J. 11, 1511–1520. https://doi.org/10.1038/ismej.2017.16.

Huang, S.S., Tian, Y., Wang, Y.J., García, P., Liu, B.H., Lu, R., Wu, L.T., Bao, H.D., Pang, M.D., Zhou, Y., Wang, R., Zhang, H., 2022. The broad host range phage vB_CpeS_BG3P is able to inhibit *Clostridium perfringens* growth. Viruses 14, 676. https://doi.org/10.3390/v14040676.

Hu, Z.M., Chen, X.Y., Chen, W.Y., Li, P., Bao, C.J., Zhu, L.G., Zhang, H.Y., Dong, C., Zhang, W., 2021. Siphoviridae phage PH669 capable of iysing some strains of O3 and O4 serotypes in *Vibrio parahaemolyticus*. Aquaculture 545, 737192. https://doi.org/10.1016/j.aquaculture.2021.737192.

Hyde, J.R., Armond, T., Herring, J.A., Hope, S., Grose, J.H., Breakwell, D.P., Pickett, B.E., 2024. Diversity and conservation of the genome architecture of phages infecting the Alphaproteobacteria. Microbiol. 12, e02827 https://doi.org/10.1128/spectrum.02827-23.

Jeon, G., Ahn, J., 2020. Assessment of phage-mediated inhibition of *Salmonella Typhimurium* treated with sublethal concentrations of ceftriaxone and ciprofloxacin. FEMS Microbiol. Lett. 367, 159. https://doi.org/10.1093/femsle/fnaa159.

Jeon, G., Ahn, J., 2021. Evaluation of phage adsorption to *Salmonella Ttyphimurium* exposed to different levels of pH and antibiotic. Microb. Pathog. 150, 104726 https://doi.org/10.1016/j.micpath.2020.104726.

Kieft, K., Anantharaman, K., 2022. Deciphering active prophages from metagenomes. mSystems 7, e0008422. https://doi.org/10.1128/msystems.00084-22.

Kondo, K., Kawano, M., Sugai, M., 2021. Distribution of antimicrobial resistance and virulence genes within the prophage-associated regions in nosocomial pathogens. mSphere 6, e00452. https://doi.org/10.1128/msphere.00452-21, 21.

Köppen, K., Prensa, G.I., Rydzewski, K., Tlapák, H., Holland, G., Heuner, K., 2021. First description of a temperate bacteriophage (vB *FhiM* KIRK) of *Francisella hispaniensis* strain 3523. Viruses 13, 327. https://doi.org/10.3390/v13020327.

Krasowska, A., Biegalska, A., Augustyniak, D., Los, M., Richert, M., Lukaszewicz, M., 2015. Isolation and characterization of phages infecting *Bacillus subtilis*. BioMed Res. Int. 2015, 179597 https://doi.org/10.1155/2015/179597.

Kubo, Y., Sriyam, S., Nakagawa, R., Kimura, K., 2018. A survey of phage contamination in natto-producing factories and development of phage-resistant *Bacillus subtilis*

(natto) strains. Food Sci. Technol. Res. 24, 485–492. https://doi.org/10.3136/fstr.24.485.
Leprince, A., Mahillon, J., 2023. Phage adsorption to gram-positive bacteria. Viruses 15, 196. https://doi.org/10.3390/v15010196.
Li, C., Yuan, X.M., Li, N., Wang, J., Yu, S.B., Zeng, H.Y., Zhang, J.M., Wu, Q.P., Ding, Y., 2020. Isolation and characterization of *Bacillus cereus* phage vB_BceP-DLc1 reveals the largest member of the Φ29-like phages. Microorganisms 8, 1750. https://doi.org/10.1016/j.mtener.2020.100563.
Linares, R., Arnaud, C.A., Degroux, S., Schoehn, G., Breyton, C., 2020. Structure, function and assembly of the long, flexible tail of siphophages. Curr. Opin. Virol. 45, 34–42. https://doi.org/10.1016/j.coviro.2020.06.010.
Li, P., Lin, H., Mi, Z.Q., Xing, S.Z., Tong, Y.G., Wang, J.X., 2019. Screening of polyvalent phage- resistant *Escherichia coli* strains based on phage receptor analysis. Front. Microbiol. 10, 850. https://doi.org/10.3389/fmicb.2019.00850.
Liu, M., Bischoff, K.M., Gill, J.J., Mire-Criscione, M.D., Berry, J.D., Young, R., Summer, E. J., 2015. Bacteriophage application restores ethanol fermentation characteristics disrupted by *Lactobacillus fermentum*. Biotechnol. 8, 1–13. https://doi.org/10.1186/s13068-015-0325-9.
Lu, H., Yan, P.H., Xiong, W.B., Wang, J.W., Liu, X.C., 2020. Genomic characterization of a novel virulent phage infecting *Shigella fiexneri* and isolated from sewage. Virus Res. 283, 197983 https://doi.org/10.1016/j.virusres.2020.197983.
Lv, R.R., Gao, X., Zhang, C., Lian, W.Q., Quan, X.Y., Guo, S., Chen, X., 2023a. Characteristics and whole-genome analysis of *Limosilactobacillus fermentum* phage LFP02. Foods 12, 2716. https://doi.org/10.3390/foods12142716.
Lv, R.R., Xu, M., Guo, S., Yao, J.W., Sakandar, H.A., Guo, J., Zhang, C., Chen, X., 2023b. Characterization of a novel *Bacillus methylotrophicus* phage BM-P1. Food Qual. Saf. 7, 1–10. https://doi.org/10.1093/fqsafe/fyad016.
Mahony, J., Alqarni, M., Stockdale, S., Spinelli, S., Feyereisen, M., Cambillau, C., Sinderen, D.V., 2016. Functional and structural dissection of the tape measure protein of *Lactococcal* phage TP901-1. Sci. Rep. 6, 36667. https://www.nature.com/articles/srep36667.
Mercanti, D.J., Ackermann, H.W., Quiberoni, A., 2015. Characterization of two temperate *Lactobacillus paracasei* bacteriophages: morphology, kinetics and adsorption. Intervirology 58, 49–56. https://doi.org/10.1159/000369207.
Oechslin, F., Zhu, X.J., Dion, M.B., Shi, Z., Moineau, S., 2022. Phage endolysins are adapted to specific hosts and are evolutionarily dynamic. PLoS Biol. 20, e3001740 https://doi.org/10.1371/journal.pbio.3001740.
Pei, Z.M., Sadiq, F.A., Han, X., Zhao, J.X., Zhang, H., Ross, R.P., Lu, W.W., Chen, W., 2020. Identification, characterization, and phylogenetic analysis of eight new inducible prophages in *lactobacillus*. Virus Res. 286, 198003 https://doi.org/10.1016/j.virusres.2020.198003.
Pell, L.G., Kanelis, V., Donaldson, L.W., Howell Lynne, P., Davidson, A.R., 2009. The phage λ major tail protein structure reveals a common evolution for long-tailed phages and the type VI bacterial secretion system. P. Natl. Acad. Sci. 106, 4160–4165. https://doi.org/10.1073/pnas.0900044106.
Pujato, S.A., Mercanti, D.J., Guglielmotti, D.M., Rousseau, G.M., Moineau, S., Reinheimer, J.A., Quiberoni, A.L., 2015. Phages of dairy *Leuconostoc mesenteroides*: genomics and factors influencing their adsorption. Int. J. Food Microbiol. 201, 58–65. https://doi.org/10.1016/j.ijfoodmicro.2015.02.016.
Sachetti, C., Tonial, F., Omidian, H., Rossato-Grando, L.G., Goelzer, C.F., Spassim, M.R., Bertol, C.D., 2021. Isothermal degradation kinetics of the probiotic *Lactobacillus fermentum* by thermogravimetry. J. Therm. Anal. Calorim. 146, 2543–2547. https://doi.org/10.1007/s10973-021-10557-0.
Shan, X.Y., Szabo, R.E., Cordero, O.X., 2023. Mutation-induced infections of phage-plasmids. Nat. Commun. 14, 2049. https://doi.org/10.1038/s41467-023-37512-x.
Silva, J.B., Storms, Z., Sauvageau, D., 2016. Host receptors for bacteriophage adsorption. FEMS Microbiol. Lett. 363, fnw002 https://doi.org/10.1093/femsle/fnw002.
Stachurska, X., Roszak, M., Jabłońska, J., Mizielińska, M., Nawrotek, P., 2021. Double-layer agar (DLA) modifications for the first step of the phage-antibiotic synergy (PAS) identification. Antibiotics 10, 1306. https://doi.org/10.3390/antibiotics10111306.
Sun, S.Y., Gao, S., Kondabagil, K., Xiang, Y., Rossmann, M.G., Rao, V.B., 2012. Structure and function of the small terminase component of the DNA packaging machine in T4-like bacteriophages. P. Natl. Acad. Sci. 109, 817–822. https://doi.org/10.1073/pnas.1110224109.
Sunthornthummas, S., Doi, K., Rangsiruji, A., Sarawaneeyaruk, S., Pringsulaka, O., 2017. Isolation and characterization of *Lactobacillus paracasei* LPC and phage ΦT25 from fermented milk. Food Control 73, 1353–1361. https://doi.org/10.1016/j.foodcont.2016.10.052.
Thanki, A.M., Taylor-Joyce, G., Dowah, A., Nale, J.Y., Malik, D., Clokie, M.R.J., 2018. Unravelling the links between phage adsorption and successful infection in *Clostridium difficile*. Viruses 10, 411. https://doi.org/10.3390/v10080411.
Toit, A.D., 2019. Phage induction in different contexts. Nat. Rev. Microbiol. 17, 126–127. https://doi.org/10.1038/s41579-019-0150-4.
Trucco, V., Reinheimer, J., Quiberoni, A., Suárez, V.B., 2011. Adsorption of temperate phages of *Lactobacillus delbrueckii* strains and phage resistance linked to their cell diversity. J. Appl. Microbiol. 110, 935–942. https://doi.org/10.1111/j.1365-2672.2011.04945.x.
Wang, J.Q., Deng, J., Du, E.D., Guo, H.G., 2022. Reevaluation of radical-induced differentiation in UV-based advanced oxidation processes (UV/hydrogen peroxide, UV/peroxydisulfate, and UV/chlorine) for metronidazole removal: kinetics, mechanism, toxicity variation, and DFT studies. Sep. Purif. Technol. 301, 121905 https://doi.org/10.1016/j.seppur.2022.121905.
Wang, S., Kong, J., Zhang, X., 2008. Identification and characterization of the two-component cell lysis cassette encoded by temperate bacteriophage ΦPYB5 of *Lactobacillus fermentum*. J. Appl. Microbiol. 105, 1939–1944. https://doi.org/10.1111/j.1365-2672.2008.03953.x.
Xu, M., Ma, R.R., Zhang, C., Huang, X.C., Gao, X., Lv, R.R., Chen, X., 2023. Inactivation of *Lactobacillus* bacteriophages by dual chemical treatments. Pol. J. Microbiol. 72, 21–28. https://doi.org/10.33073/pim-2023-004.
Ye, Y.M., Chen, H.F., Huang, Q.L., Huang, S.X., He, J.X., Zhang, J.M., Wu, Q.P., Li, X.L., Hu, W.F., Yang, M.Y., 2022. Characterization and genomic analysis of novel *Vibrio parahaemolyticus* phage vB_VpaP_DE10. Viruses 14, 1609. https://doi.org/10.3390/v14081609.
Yoon, B.H., Chang, H.I., 2011. Complete genomic sequence of the *Lactobacillus* temperate phage LF1. Arch. Virol. 156, 1909–1912. https://doi.org/10.1007/s00705-011-1082-0.
Yuan, L., Fan, L.Y., Zhao, H.Y., Mgomi, F.C., Ni, H., He, G.Q., 2022. RNA-seq reveals the phage-resistant mechanisms displayed by *Lactiplantibacillus plantarum* ZJU-1 isolated from Chinese traditional sourdough. Int. Dairy J. 127, 105286 https://doi.org/10.1016/j.idairyj.2021.105286.
Zaburlin, D., Quiberoni, A., Mercanti, D., 2017. Changes in environmental conditions modify infection kinetics of dairy phages. Food Environ. Virol. 9, 270–276. https://doi.org/10.1007/s12560-017-9296-2.
Zago, M., Bonvini, B., Rossetti, L., Meucci, A., Giraffa, G., Carminati, D., 2015. Biodiversity of *Lactobacillus helveticus* bacteriophages isolated from cheese whey starters. J. Dairy Res. 82, 242–247. https://doi.org/10.1017/S0022029915000151.
Zampara, A., Sørensen, M.C.H., Grimon, D., Antenucci, F., Vitt, A.R., Bortolaia, V., Briers, Y., Brøndsted, L., 2020. Exploiting phage receptor binding proteins to enable endolysins to kill gram-negative bacteria. Sci. Rep. 10, 12087. https://www.nature.com/articles/s41598-020-68983-3.
Zhang, K.L., Pankratz, K., Duong, H., Theodore, M., Guan, J.W., Jiang, A., Lin, Y.R., Zeng, L.Y., 2021. Interactions between viral regulatory proteins ensure an MOI-independent probability of lysogeny during infection by bacteriophage P1. NLM 12, e01013–e01021. https://doi.org/10.1128/mbio.01013-21.
Zhang, L., Ma, H., Kulyar, M.F., Pan, H., Li, K., Li, A., Mo, Q., Wang, Y., Dong, H., Bao, Y., Li, J., 2021. Complete genome analysis of *Lactobacillus fermentum* YLF016 and its probiotic characteristics. Microb. Pathog. 162, 105212 https://doi.org/10.1016/j.micpath.2021.105212.
Zhang, X., Lan, Y., Jiao, W.C., Li, Y.J., Tang, L.J., Jiang, Y.P., Cui, W., Qiao, X.Y., 2015. Isolation and characterization of a novel virulent phage of *Lactobacillus casei* ATCC 393. Food Environ. Virol. 7, 333–341. https://doi.org/10.1007/s12560-015-9206-4.
Zhang, Y.J., Liao, Y.T., Salvador, A., Sun, X.H., Wu, V.C.H., 2020. Prediction, diversity, and genomic analysis of temperate phages induced from shiga toxin-producing *Escherichia coli* strains. Front. Microbiol. 10, 3093. https://doi.org/10.3389/fmicb.2019.03093.
Zhao, Y., Hong, K., Zhao, J.X., Zhang, H., Zhai, Q.X., Chen, W., 2019. *Lactobacillus fermentum* and its potential immunomodulatory properties. J. Funct.Foods 56, 21–32. https://doi.org/10.1016/j.jff.2019.02.044.
Zhu, H.F., Guo, S., Zhao, J., Hafiz, A.S., Lv, R.R., Wen, Q.N., Chen, X., 2022. Whole genome sequence analysis of *Lactiplantibacillus plantarum* bacteriophage P2. Pol. J. Microbiol. 71, 421–428. https://doi.org/10.33073/pjm-2022-037.